

Supplementary Materials for
**Quantitative immunopeptidomics reveals a tumor stroma–specific target for
T cell therapy**

Gloria B. Kim *et al.*

Corresponding author: Toni Weinschenk, toni.weinschenk@immatics.com; James L. Riley, rileyj@upenn.edu

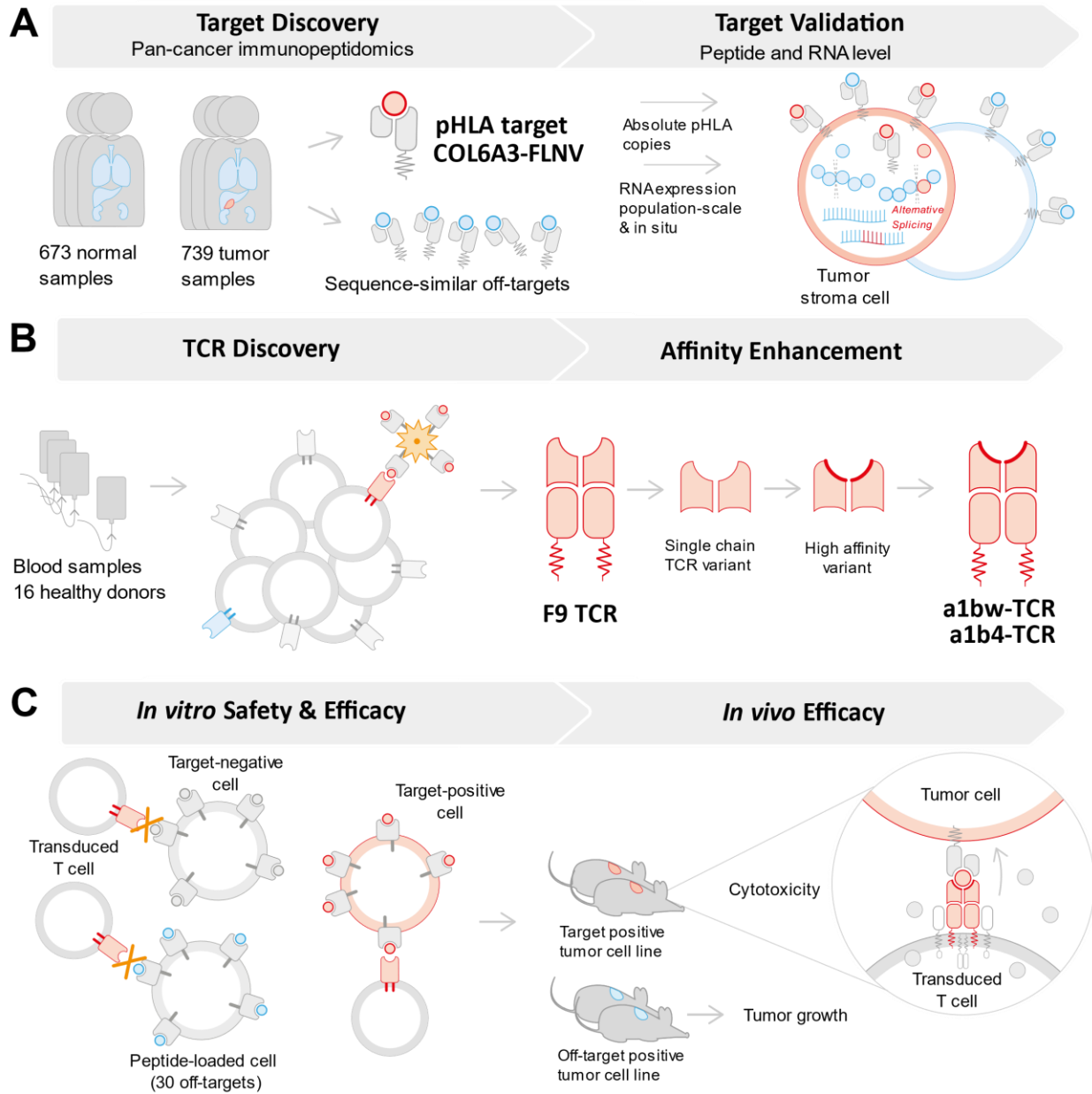
Sci. Transl. Med. **14**, eabo6135 (2022)
DOI: 10.1126/scitranslmed.abo6135

The PDF file includes:

Figs. S1 to S8
Tables S1 to S4

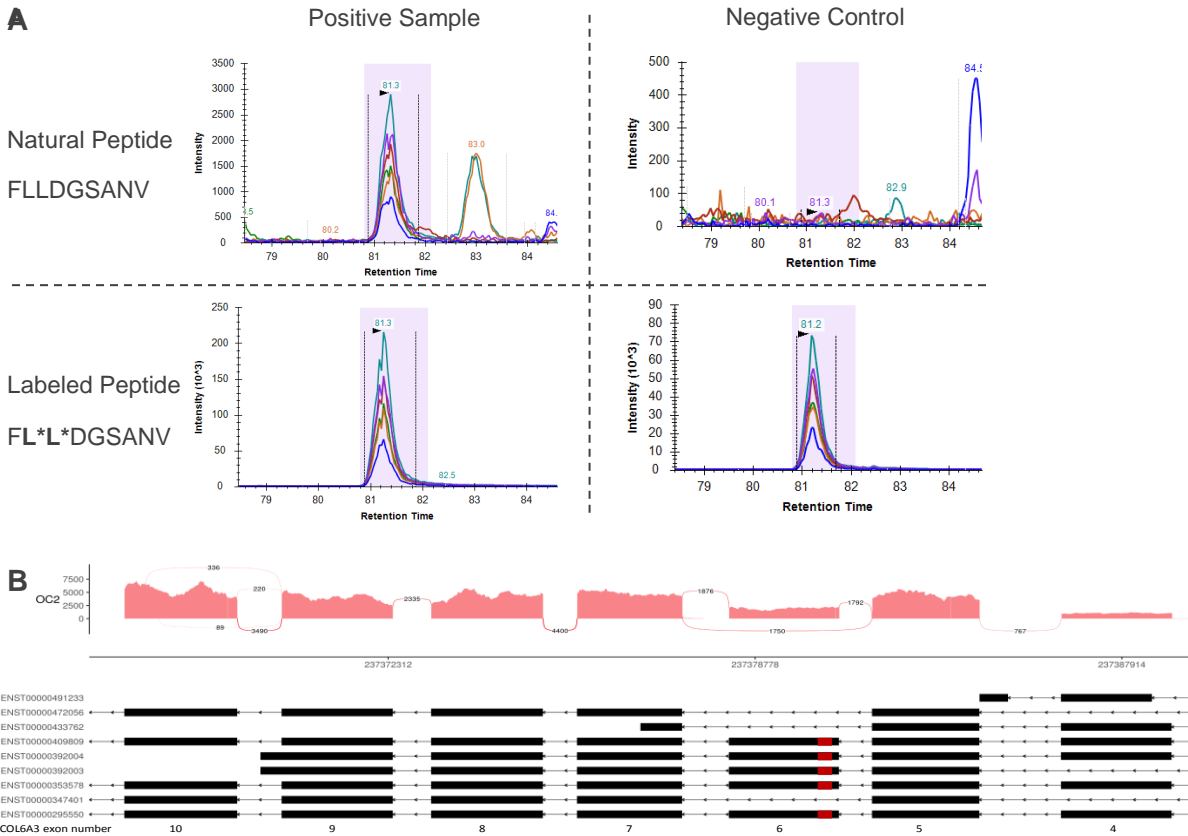
Other Supplementary Material for this manuscript includes the following:

MDAR Reproducibility Checklist

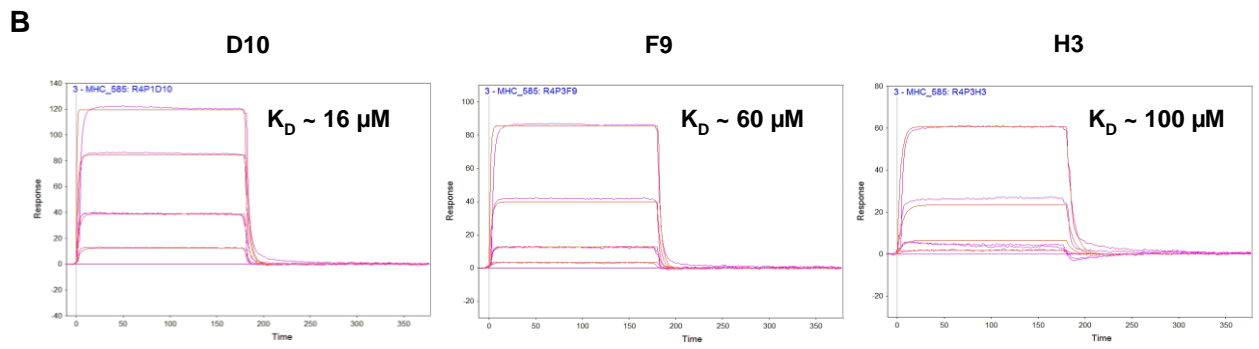
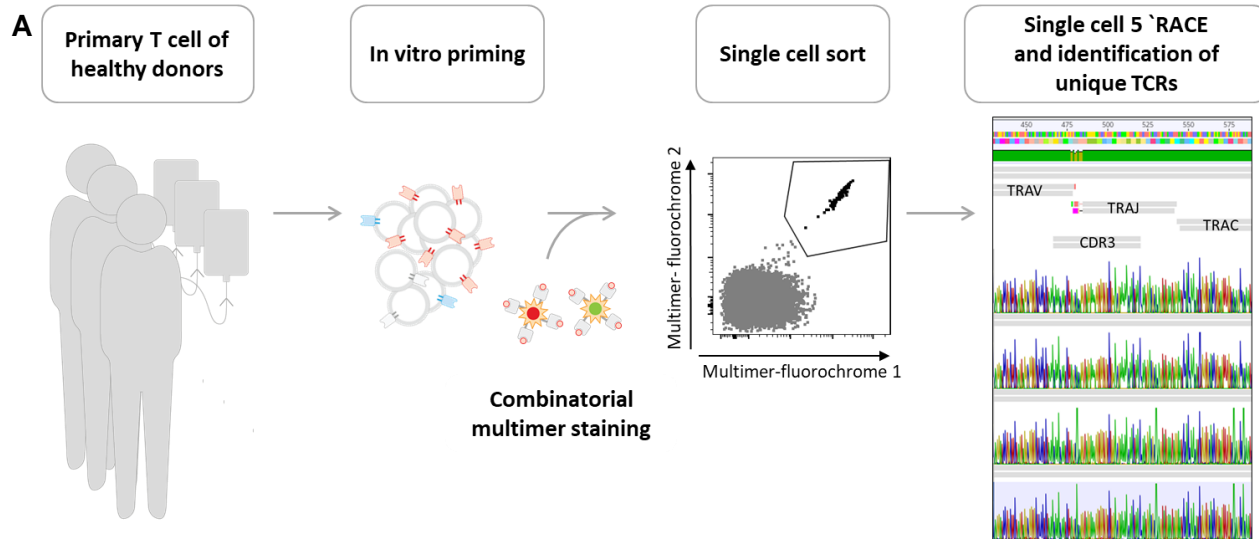


Supplementary Figure 1. Schematic outline summarizing the discovery and validation of a HLA-restricted cancer target and TCRs suitable for adoptive T cell therapy. Three phases are highlighted starting with target discovery and validation, TCR discovery and engineering and finally preclinical in vitro and in vivo efficacy and safety studies. **(A)** Target discovery is based on pan-cancer population-scale immunopeptidomics identifying tumor-specific HLA-A*02 peptide targets together with potential off-targets used in TCR discovery as counter targets and for in vitro safety studies. Target validation contributed additional target characteristics about mRNA splicing (RNA-sequencing), absolute copy numbers (targeted mass spectrometry) and stroma association (in situ hybridization). **(B)** Suitable TCRs were extracted from blood of healthy donors incorporating early screening of sequence similar counter targets identified by immunopeptidomics in the first step. TCR F9 with favorable characteristics was engineered into two soluble and high affinity variants. **(C)** Preclinical safety and efficacy were finally

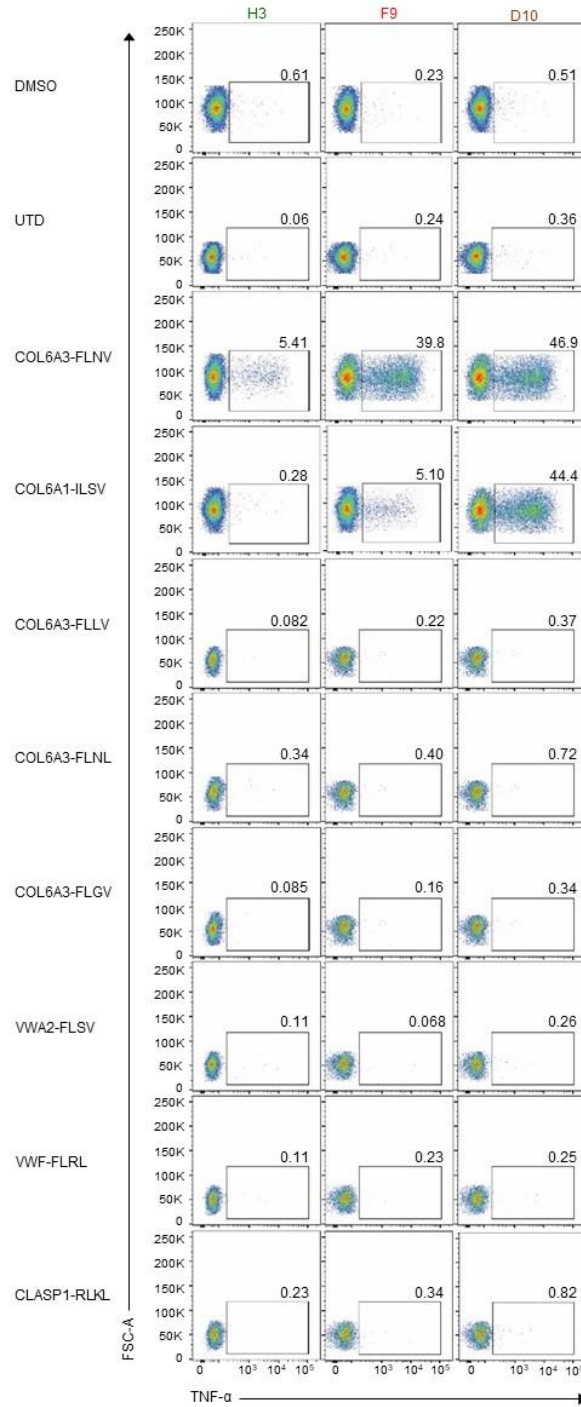
assessed by use of target negative and positive cell lines as well as cell lines loaded with 30 sequence similar peptides. Finally, in vivo efficacy in mouse models was evaluated.



Supplementary Figure 2. Validation of COL6A3-FLNV sequence and alternative splicing of exon 6. (A) Verification of COL6A3-FLNV peptide sequence by co-elution with stable isotope labeled internal control on ovarian cancer sample OC2. Adrenal gland from a healthy donor was used as negative control. **(B)** Sashimi plots for an ovarian cancer sample OC2 illustrating read coverage for individual exons and exon spanning reads that prove alternative splicing events. COL6A3 ENSEMBL annotation is depicted below indicating the position of the COL6A3-FLNV peptide as red squares.

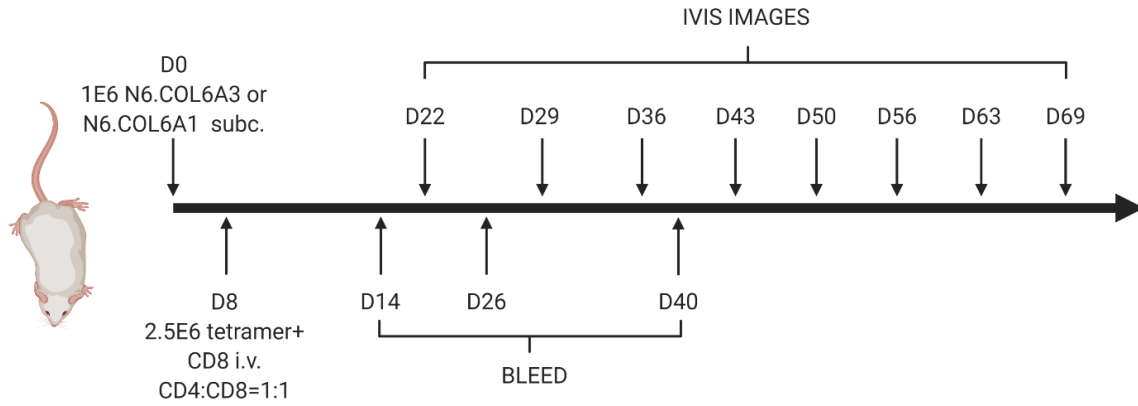
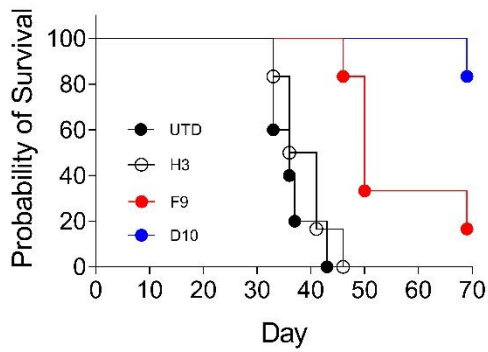
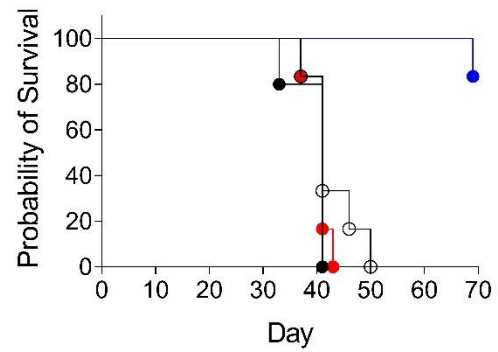


Supplementary Figure 3. Discovery and characterization of natural COL6A3-specific TCRs. (A) Summary of the TCR discovery process. **(B)** Surface plasmon resonance (SPR) analysis for binding affinity determination of TCRs, D10, F9, and H3. COL6A3-FLNV in complex with biotinylated HLA-A*02:01 was immobilized on streptavidin SPR chips and soluble TCR variants of D10, F9, and H3 were applied at concentrations of 0 μM , 1.6 μM , 6.3 μM , 25 μM , and 100 μM , respectively. Binding equilibrium dissociation constants (K_D) of 16 μM , 60 μM , and 100 μM were determined for D10, F9, and H3, respectively.

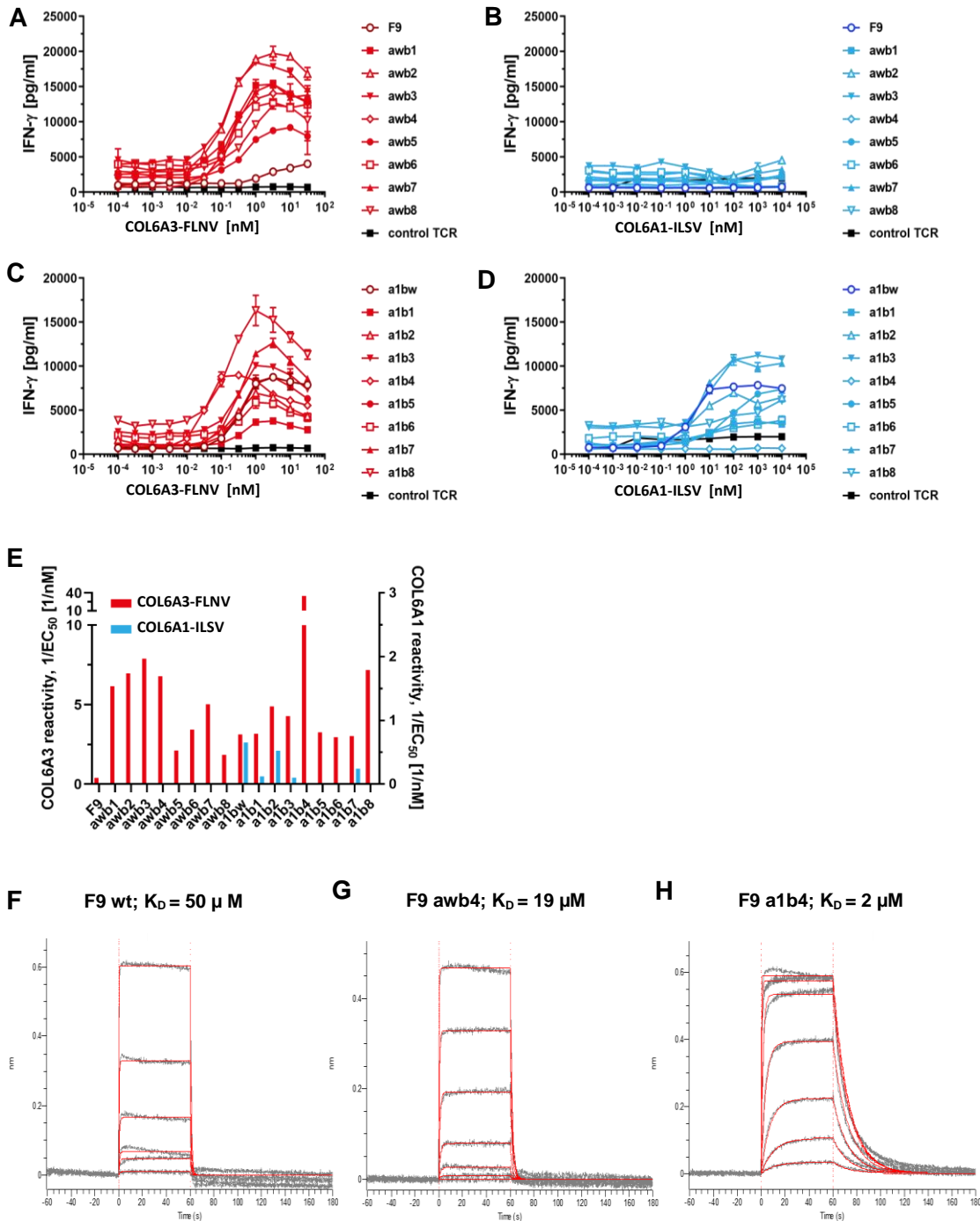


Supplementary Figure 4. Characterization of TCR specificity using naturally presented similar peptides.

T cells were mixed with the indicated peptide-loaded K.A2 cells for 4 hours and TNF α intracellular staining is shown for CD8 T cells. Results are representative of three independent experiments with different donors performed in triplicate. Peptide concentrations used were all 10 μ M.

A**B N6.COL6A3****C N6.COL6A1**

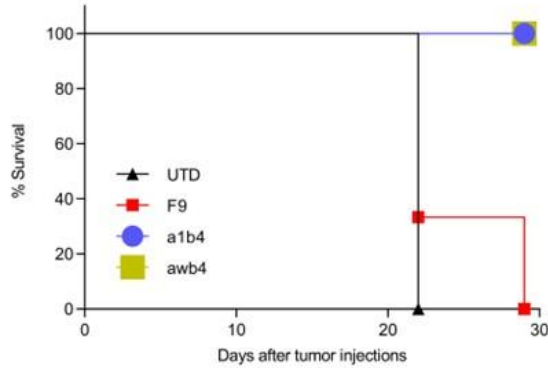
Supplementary Figure 5. Natural COL6A3-specific TCRs confer limited anti-tumor immunity in vivo. (A) Timeline of in vivo experiment performed on NSG mice implanted with N6.COL6A3 or N6.COL6A1 cells. Survival curves of N6.COL6A3 group (**B**) and N6.COL6A1 group (**C**).



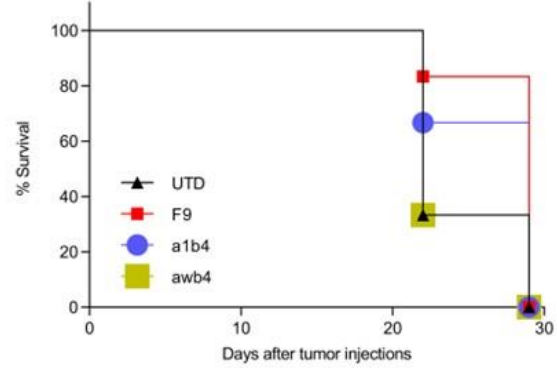
Supplementary Figure 6. Characterization of affinity-enhanced TCRs. EC_{50} determination for reactivity of TCRs with mutations in beta chain against COL6A3-FLNV (**A**) and COL6A1-ILSV (**B**). EC_{50} determination for reactivity of TCRs with alpha chain mutation combined with mutations in beta chain against COL6A3-FLNV (**C**) and COL6A1-ILSV (**D**). (**E**) Fold change in COL6A3 and COL6A1 reactivity for matured TCR variants compared to F9 variant, (**F-H**) Biolayer interferometry (BLI) analysis for affinity determination of TCR F9 and its matured variants Fawb4 and a1b4. COL6A3-FLNV in complex with biotinylated HLA-A*02:01 was immobilized on streptavidin BLI sensors and soluble TCR variants of F9, awb4 and a1b4 were applied at concentrations of 0.1 μM , 0.3 μM , 1 μM , 3.2 μM , 10 μM , 31.6 μM and 100 μM , respectively. Binding

equilibrium dissociation constants (K_D) of approximately 50 μ M, 20 μ M and 2 μ M were determined for F9, awb4 and a1b4, respectively.

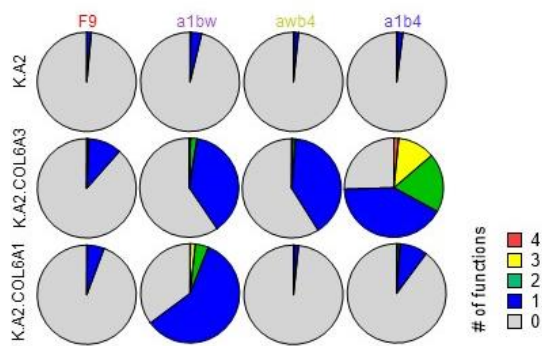
A K.A2.COL6A3



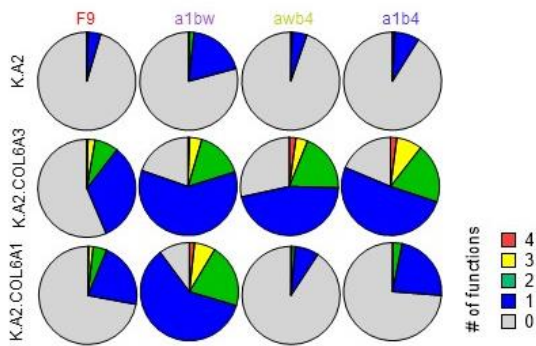
B K.A2.COL6A1



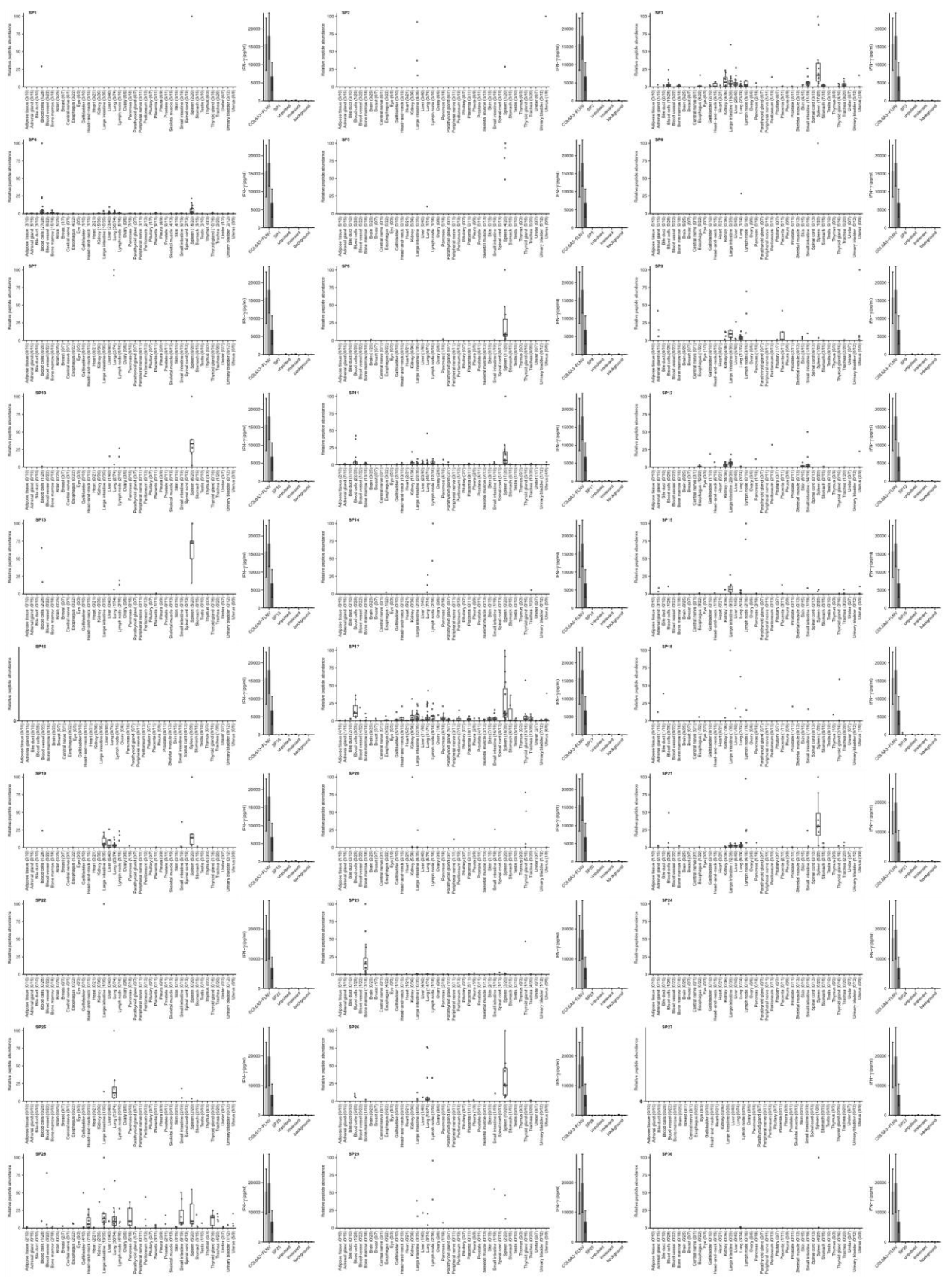
C Gated on live CD4+ T cells



D Gated on live CD8+ T cells



Supplementary Figure 7. Survival curves of mice treated with affinity enhanced COL6A3 TCRs and polyfunctional analysis of COL6A3-specific T cells at the end of experiment. Survival curves of K.A2.COL6A3 group (A) and K.A2.COL6A1 group (B) from the study described in Fig 6. Pie charts representing the number of cytokines CD4+ (C) or CD8+ (D) T cells produce.



Supplementary Figure 8. Peptide presentation and TCR reactivity for 30 similar peptides. Relative abundance of HLA-bound peptides similar to COL6A3-FLVN isolated from normal samples. Each dot represents the median from five technical replicates of samples for which the peptide was detected and quantified. The number of donors with peptide detection as well as the total number per group is indicated in parentheses. Next to the data for each peptide is a bar graph showing the amount of IFN- γ produced when TCR-transduced T cells [F9 (light gray), awb4 (gray) and a1b4 (dark gray)] were incubated with peptide-loaded T2 cells. Error bars represent the standard deviation of three biological replicates.

Supplementary Table 1. Differential expression analysis for COL6A3-FLNV by relative peptide quantitation using mass-spectrometry and exon expression analysis of COL6A3-E6 by mRNA-sequencing. Fold changes within the different tumor indications are determined with respect to average abundance on healthy tissues. The average abundance was computed by first determining the median abundances within each organ followed by using the geometric mean across all organs. If the peptide was not detected for the given tumor indication, no fold change could be determined indicated by “n.a.”.

Tumor indication	Relative Peptide Quantitation COL6A3-FLNV			Exon Expression COL6A3-E6		
	Fold Change	Number of samples	p-value (corrected)	Fold Change	Number of samples	p-value (corrected)
Acute myeloid leukemia	n.a.			0.0	22	1.0E+00
Breast cancer	22.6	22	6.7E-10	8.3	15	2.7E-06
Cholangiocellular carcinoma	22.3	5	1.5E-04	21.1	4	5.7E-02
Chronic lymphatic leukemia	n.a.			0.0	11	
Colorectal cancer	3.0	16	5.7E-05	5.1	38	1.2E-06
Esophageal cancer	23.0	13	5.5E-06	13.4	41	6.8E-14
Gallbladder cancer	9.5	4	2.0E-02	9.0	6	1.3E-02
Gastric cancer	10.4	8	7.3E-05	4.6	18	1.1E-05
Gastroesophageal junction cancer	1.7	2	4.1E-01	0.4	1	
Glioblastoma multiforme	n.a.			1.2	24	7.9E-01
Head-and-neck squamous cell carcinoma	9.0	15	2.1E-05	9.7	43	3.3E-12
Hepatocellular carcinoma	2.5	2	3.1E-01	0.6	41	1.0E+00
Lung adenocarcinoma	17.8	34	8.2E-17	7.5	56	8.0E-17
Melanoma	5.1	4	5.6E-02	8.2	10	1.6E-03
Non-Hodgkin-Lymphoma	2.8	3	4.9E-01	1.6	14	6.2E-01
Other non-small cell lung ca.	11.3	13	2.1E-05	13.7	5	4.5E-03
Ovarian cancer	11.0	13	9.5E-05	4.9	36	1.0E-10
Pancreatic cancer	13.8	8	6.0E-05	8.2	26	8.3E-09
Prostate cancer	n.a.			1.2	20	1.9E-01
Renal cell carcinoma	8.7	2	7.0E-02	0.6	15	1.0E+00
Small cell lung carcinoma	18.5	11	2.3E-07	6.0	13	4.4E-05
Squamous cell lung carcinoma	22.3	25	4.9E-12	13.9	45	1.2E-22
Urinary bladder cancer	5.4	6	2.6E-02	2.1	11	1.0E-01
Uterus endometrial cancer	2.7	4	1.5E-01	2.5	14	8.8E-02

Supplementary Table 2. Microscopic evaluation of *COL6A3-E6* RNA expression determined by in situ hybridization in cancer samples from pancreas cancer (PC), colorectal cancer (CRC), breast cancer (BRCA), ovarian cancer (OC), gastric cancer (GC), head-and-neck squamous cell cancer (HNSCC), non-small cell lung carcinoma (NSCLC) and esophageal cancer (EC). Staining intensity (SI) in stroma or tumor cells was assessed as dots per cell and the pre-dominant phenotype was categorized in SI scores ranging from 0 to 4. The frequency of stroma or tumor cells showing the pre-dominant SI score was estimated in percent and categorized as percent points (PP) from 0 to 4. For each sample a combined immunoreactive score (IRS) was calculated for stroma and tumor cells respectively as follows: IRS = SI x PP.

Tissues (n=30)	COL6A3-E6 FPKM	Stroma area			Tumor area		
		Signal Intensity [SI]	Percent positive stroma cells [PP]	combined IRS	Signal Intensity [SI]	Percent positive tumor cells [PP]	combined IRS
PC1	n/a	SI3	60 %	IRS 9	0	0	0
CRC1	0.76	SI2	60 %	IRS 6	0	0	0
BRCA1	0.88	SI3-4	51 %	IRS9-12	0	0	0
EC1	0.89	SI4	>95 %	IRS16	0	0	0
BRCA2	1.20	SI4	75 %	IRS12	0	0	0
BRCA3	1.70	SI3	81 %	IRS12	0	0	0
HNSCC1	2.59	SI4	90 %	IRS 16	0	0	0
BRCA4	3.11	SI4	66 %	IRS 12	0	0	0
NSCLC1	3.58	SI2	60 %	IRS 6	0	0	0
BRCA5	3.91	SI4	60 %	IRS 12	SI1	5 %	IRS 1
BRCA6	4.04	SI4	81 %	IRS 16	SI1	33 %	IRS 2
OC1	4.04	SI3	81 %	IRS 12	0	0	0
NSCLC2	4.23	SI2	79 %	IRS 6	0	0	0
NSCLC3	4.88	SI4	66 %	IRS 12	0	0	0
EC2	5.92	SI3	70 %	IRS 9	0	0	0
HNSCC2	6.22	SI4	90 %	IRS 16	0	0	0
HNSCC3	6.45	SI4	90 %	IRS 16	0	0	0
NSCLC4	6.53	SI3	49 %	IRS 6	0	0	0
BRCA7	7.47	SI4	66 %	IRS 12	0	0	0
EC3	8.72	SI4	90 %	IRS 16	0	0	0
EC4	10.17	SI4	90 %	IRS 16	0	0	0
NSCLC5	10.68	SI3	60 %	IRS 9	0	0	0
NSCLC6	10.96	SI4	90 %	IRS 16	0	0	0
GC1	12.36	SI3	75 %	IRS 9	0	0	0
NSCLC7	17.02	SI4	100 %	IRS 16	SI2	50 %	IRS 4
HNSCC4	24.61	SI4	95 %	IRS 16	0	0	0
NSCLC8	25.95	SI4	90 %	IRS 16	0	0	0
EC5	27.75	SI4	90 %	IRS 16	SI1	10 %	IRS 1
NSCLC9	30.04	SI4	90 %	IRS 16	0	0	0
HNSCC5	51.30	SI4	>95 %	IRS 16	0	0	0

Immunoreactivity score (IRS)						
SI x PP = IRS						
(SI) Signal intensity	Percent Points (PP)	SI0	SI1	SI2	SI3	SI4
		0 (dots/cell)	1-3 (dots/cell)	4-9 (dots/cell)	10-15 (dots/cell)	>15 or cluster
PP0	0 %	0	0	0	0	0
PP1	1-10 %	0	1	2	3	4
PP2	11-50 %	0	2	4	6	8
PP3	51-80 %	0	3	6	9	12
PP4	>80 %	0	4	8	12	16

Supplementary Table 3. Characterized TCRs with IMGT identifier of variable alpha (TRAV), joining alpha (TRAJ), variable beta (TRBV) and joining beta chain (TRBJ) as well as sequences for complementarity-determining regions.

TCR	TRAV	TRAJ	TRBV	TRBJ	CDRa1	CDRa3	CDRb1	CDRb3
D10	12-2*01	30*01	9*02	1-2*01	DRGSQS	AVNFHDKII	RSGDLS	ASSVASAYGYT
H3	12-2*01	49*01	7-8*01	2-1*01	DRGSQS	AVKAGNQFY	ISGHVS	ASSLLTSGGDNEQF
F9	12-2*01	28*01	9*01	1-2*01	DRGSQS	AAYSGAGSYQLT	RSGDLS	ASSVESSYGYT
a1bw	12-2*01	28*01	9*01	1-2*01	DRRSQS	AAYSGAGSYQLT	RSGDLS	ASSVESSYGYT
awb4	12-2*01	28*01	9*01	1-2*01	DRGSQS	AAYSGAGSYQLT	AMDHPY	ASSVESSYGYT
a1b4	12-2*01	28*01	9*01	1-2*01	DRRSQS	AAYSGAGSYQLT	AMDHPY	ASSVESSYGYT

Supplementary Table 4. Similar peptides used for TCR characterization and affinity engineering. Gene symbol and description as well as the protein position of the used peptides is listed. Positions with amino acids identical to the target peptide COL6A3-FLNV are highlighted in red.

Gene symbol	Gene description	Peptide sequence	Peptide name	Source protein and position
COL6A1	collagen, type VI, alpha 1	ILLDGSASV	COL6A1-ILSV	P12109 p832-840
COL6A3	collagen, type VI, alpha 3	FLFDGSANL	COL6A3-FLNL	P12111 p840-848
		FLFDGSANLV	COL6A3-FLLV	P12111 p840-849
		FLLDGSEGV	COL6A3-FLGV	P12111 p1032-1040
VWA2	von Willebrand factor A domain containing 2	FLLDGSNSV	VWA2-FLSV	Q5GFL6 p54-62
VWF	von Willebrand factor	FLLDGSSRL	VWF-FLRL	P04275 p1280-1288
CLASP1	cytoplasmic linker associated protein 1	RLLDGAFLK	CLASP1-RLKL	Q7Z460 p367-375